

The radio flaring behaviour of GRO J1655 – 40: an analogy with extragalactic radio sources?

J. A. Stevens^{1,2}, D. C. Hannikainen^{3,4}, Kinwah Wu^{2,5}, R. W. Hunstead⁵ and D. J. McKay^{6,7}

¹*Astronomy Technology Centre, Royal Observatory, Blackford Hill, Edinburgh, EH9 3HJ*

²*Mullard Space Science Laboratory, University College London, Holmbury St. Mary, Surrey, RH5 6NT*

³*Department of Physics and Astronomy, University of Southampton, Southampton, SO17 1BJ*

⁴*Observatory, PO Box 14, 00014 University of Helsinki, Finland*

⁵*School of Physics A28, University of Sydney, NSW 2006, Australia*

⁶*Telescope Technologies Ltd, 1 Morpeth Wharf, Birkenhead, Merseyside CH41 1NQ*

⁷*Australia Telescope National Facility, Locked Bag 194, Narrabri, NSW 2390, Australia*

Received:

ABSTRACT

At radio frequencies, the current evidence for the microquasar–quasar connection is based on imaging observations showing that relativistic outflows/jets are found in both classes of objects. Some microquasars also display superluminal motion, further strengthening the view that microquasars are in fact Galactic miniatures of quasars. Here we demonstrate that this connection can be extended to incorporate timing and spectral observations. Our argument is based on the striking similarity found in the radio flaring behaviour of the Galactic superluminal source GRO J1655–40 and of extragalactic sources, such as the blazar 3C 273. We find that the variability of GRO J1655–40 can be explained within the framework of the successful generalised shock model for compact extragalactic radio sources in which the radio emission arises from shocked plasma in relativistic jets. Specifically, the multifrequency flare amplitudes, time delays and radio polarization position angle measurements are consistent with the predictions of the growth stage of this model.

Key words: X-rays: binaries — galaxies: jets — quasars: general — black hole physics — radiation mechanism: general — shock waves

1 INTRODUCTION

Microquasars, here defined as X-ray binaries containing a black hole accreting material from a companion star, are generally regarded as the Galactic counterparts of more powerful extragalactic radio sources, such as blazars and radio galaxies.¹ This implies that the underlying physical processes that operate in these systems are the same, and thus are manifested in their radiative properties. At radio frequencies, the main argument for microquasars being Galactic miniatures of quasars is based on imaging observations of relativistic outflows in the former. This is further strengthened by the fact that some microquasars also display superluminal motion analogous to their extragalactic counterparts. For recent reviews of

the radio properties of microquasars, see e.g. Mirabel & Rodríguez (1998, 1999) and Fender (2001, 2002).

The two unambiguous Galactic superluminal sources to date are GRS 1915+105 and GRO J1655–40. Their radio jets were discovered in the mid-1990s (Hunstead et al. 1994; Reynolds et al. 1994; Mirabel & Rodríguez 1994; Tingay et al. 1995; Hjellming & Rupen 1995). They often show radio flares during the X-ray active states, and their radio emission is polarized. The nature of GRS 1915+105 has been controversial but recent observations show that it is likely to be a low mass X-ray binary with a black-hole candidate and K-giant donor star (Greiner et al. 2001). It is certain that GRO J1655–40 is a binary system containing an evolved F-type star and a black hole (Orosz & Bailyn 1997; Soria et al. 1998).

Compact extragalactic radio sources usually show power law spectra at high-frequencies (> 90 GHz). The radio emission is of synchrotron origin, is often highly polarized, and the power law spectrum implies a non-thermal energy distribution for the relativistic electrons and an optically thin emission region. The spectra often have a turn-over at low frequencies that is generally explained as the consequence of optical-depth effects; the emission is

¹ The blazar class comprises the brightest and most variable of the extragalactic radio sources. Accordingly, for the purposes of this study, most observational data for extragalactic sources that allow comparison with the microquasars pertain to blazars. However, the ‘unified scheme’ for radio sources postulates that, to first order, the only difference between radio galaxies, quasars and blazars is one of orientation (e.g. Barthel 1989) so the same physical model should be applicable to all.

absorbed and the source becomes opaque below a certain critical frequency. The time evolution of the low-frequency (typically less than a few GHz) radio spectra was initially explained by means of a homogeneous cloud composed of relativistic electrons and magnetic field that expands adiabatically and emits synchrotron radiation (Shklovsky 1965; van der Laan 1966; Pauliny-Toth & Kellerman 1966). However, it was later found that a more satisfactory explanation is provided by models invoking shocks propagating along a relativistic jet, and hence accelerating electrons to relativistic energies (e.g. Marscher & Gear 1985; Hughes, Aller & Aller 1985, 1989a, b).

Like extragalactic radio sources, the Galactic superluminal source GRO J1655–40 also shows a power law spectrum at radio frequencies that becomes inverted during flaring (Hannikainen et al. 2000). To date the time-dependent radio properties of X-ray binaries have mostly been ascribed to the expanding-cloud (or synchrotron-bubble) model or variations thereof (Hjellming & Johnston 1988; Han & Hjellming 1992; Ball & Vlassis 1993) although an internal shock model has been applied successfully to a radio outburst of GRS 1915+105 (Kaiser, Sunyaev & Spruit 2000). Since the 1994 radio outburst of GRO J1655–40 is not readily accommodated by the expanding-cloud model (see Hannikainen et al. 2000 and Section 2 below) we propose alternatively that the processes that generate the radio emission from GRO J1655–40 and from extragalactic radio sources are the same. We make use of the shock model of Marscher & Gear (1985) to explain the spectral evolution of GRO J1655–40 during the 1994 outburst. The multifrequency variability is discussed in Section 2, basic features of the model are described in Section 3, and the quasar-microquasar connection is discussed in Section 4.

Throughout this paper, spectral index, α , is defined as $S_\nu \propto \nu^\alpha$ where S_ν is the flux density at frequency ν .

2 TIME-DEPENDENT PROPERTIES OF GRO J1655–40

GRO J1655–40 flared dramatically in 1994 August, the flux density at 843 MHz increasing from a few hundred mJy to almost 8 Jy in 12 d (Hannikainen et al. 2000). Very Long Baseline Array (VLBA) images at 1.6 GHz taken at several epochs during the outburst show well-collimated relativistic jets. The jets are resolved into several knot-like features which expand outwards from a stationary compact core (Hjellming & Rupen 1995).

The multifrequency flux density light curves and spectra (from Hannikainen et al. 2000) are shown in Figs 1 and 2 respectively. The flux densities include the emission from the entire structure shown in the VLBA images, with the possible exception of the two highest frequencies at which the Australia Telescope Compact Array (ATCA) synthesized beam size is approximately 1 arcsec compared to a source size of 1–2 arcsec at 1.6 GHz. Our flux density measurements involve fitting a point-source model to the data which may lead to a slight systematic underestimate of the flux at 8.6 and 9.2 GHz. However, the source may well be more compact at higher frequencies due to the shorter synchrotron lifetimes of the emitting electrons (see Section 4), so it is unlikely that much/any flux density is missing from our measurements. Indeed, in Section 4, we argue that most of the flux density variability is confined to a region $\ll 1$ arcsec in extent. Since the available observations do not allow separation of emission from the compact variable component(s) and the extended regions we are forced to assume that the radio emission is dominated by a single variable component. The light curves show complex flaring behaviour with

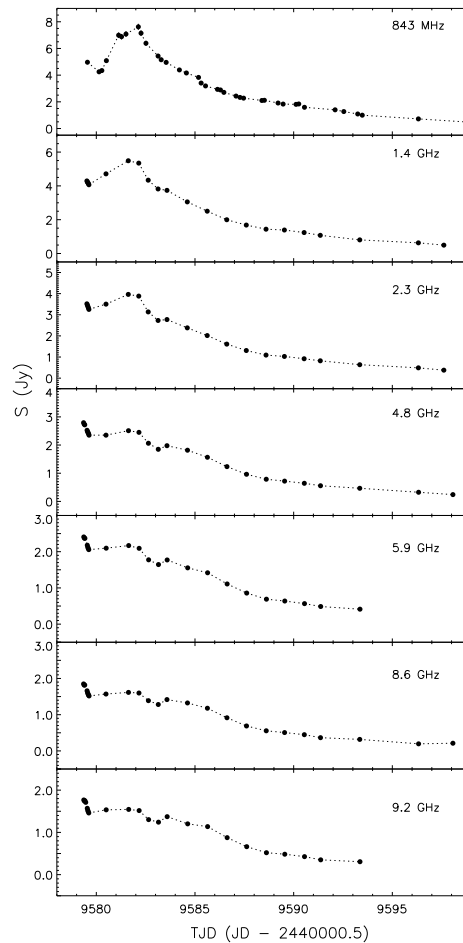


Figure 1. The multifrequency light curves of GRO J1655–40 observed by the Molonglo Observatory Synthesis Telescope (MOST; 843 MHz) and the ATCA (1.4–9.2 GHz). Data are adopted from Hannikainen et al. (2000).

several minor events following the initial increase in flux density. The key features of the data are that the initial rise in flux density *peaks simultaneously* at all frequencies and that the amplitude of the flare, defined as maximum minus minimum flux density, *increases* towards lower frequency (see Section 4 for further discussion). We quantified the time delays between the data streams with the Discrete Correlation Function (DCF; Edelson & Krolik 1988) and the Interpolated Correlation Function (ICF; Gaskell & Peterson 1987). Both methods give essentially the same result (Fig. 3); the correlation functions are approximately symmetrical around zero lag in all cases. The flat peak to the curves suggest formal time delays of $\sim 0 \pm 1$ d.

The first panel of Fig. 2 shows a spectrum from two days before flux density maximum, which is consistent with synchrotron emission that is optically thin at the highest frequencies but is partially self-absorbed at around 1 GHz. As the flux density increases, the entire spectrum becomes optically thin and remains so throughout the subsequent decline in flux density. In Fig. 2 we can see that the spectrum was relatively flat (with a spectral index of -0.41 on TJD 9580). It steepened at the time of the maximum (with the spectral indices reaching -0.65 on TJD 9582) and then flattened as the flux density declined to a level of -0.4 around TJD 9586 and 9587. This behaviour can be explained by models incorporating emission from multiple regions. In the simple core-lobe model suggested by

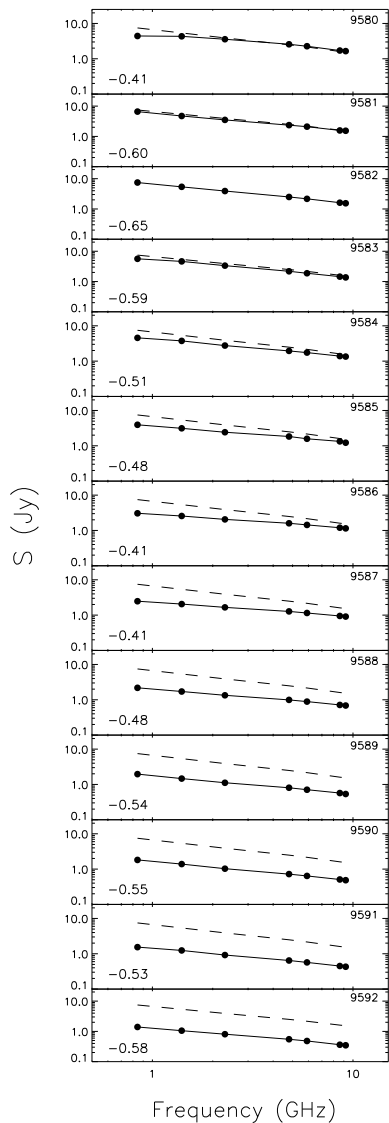


Figure 2. Spectra of GRO J1655–40 (solid lines) are shown at time intervals of one day from TJD 9580 to 9592. The data points are interpolated from the flux density light curves. The spectrum from TJD 9582 (dashed line), the epoch at which the flux density of the radio flare reached its peak, is shown for comparison. The two-point spectral indices between 843 MHz and 9.2 GHz are indicated at the bottom left of each panel. Data are adopted from Hannikainen et al. (2000).

Hannikainen et al. (2000), the observed spectrum is the sum of the emission from a compact region (core), which has a flat spectrum, and the emission from extended regions (lobes/ejecta) with steeper spectra. The outburst can be seen as a consequence of the brightening of the compact region and then the rapid rise in the brightness of the ejecta. The emission from the ejecta eventually dominates as the radio flux densities reach their peak amplitude. At the same time the spectrum steepens. As the flare subsides, the emission from the ejecta drops to a level comparable to, or lower than, the emission from the compact region, and the spectra become flatter, similar to those seen at the onset of the flare.

The time-dependent properties of the radio outbursts of GRO J1655–40 and other black-hole X-ray binaries have been attributed to synchrotron emission from expanding clouds of rel-

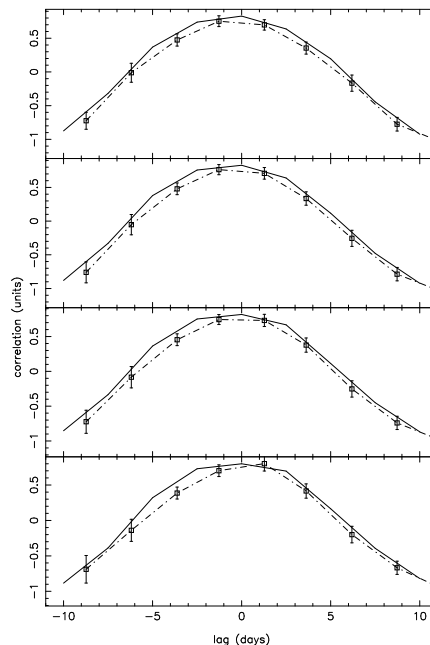


Figure 3. Application of the Discrete Correlation Function (points and dot-dashed line) and Interpolated Correlation Function (solid line) to the 9.2 GHz versus (from top to bottom) 5.9, 2.3, 1.4 and 0.843 GHz data streams.

ativistic electrons. Under the usual assumption that all radio frequencies are initially optically thick, the two major characteristics of these models are that the low-frequency emission has a time delay with respect to that at high frequencies and that the flare amplitudes fall off towards lower frequency (see e.g. Han & Hjellming 1992). The observations clearly do not conform to these predictions of the expanding-cloud model (see also Hannikainen et al. 2000).

If electrons are injected into an expanding cloud, and if expansion losses dominate over radiative losses, then it is possible to get a simultaneous peak at optically thin frequencies once the injection stops or once the expansion cooling dominates over the injection. Note that if radiative losses dominate under this scenario we would observe frequency-dependent peak times, assuming the data streams are sufficiently well sampled. However, the first panel of Fig. 3 provides evidence that the synchrotron self-absorption turnover was close to 1 GHz near the peak of the flare, implying that at least some of the radio frequencies were optically thick at earlier epochs, and thus arguing against this possibility. Similar scenarios can be produced by relaxing some of the initial assumptions of the model. For example, Ball & Vlassis (1993) considered cases where electrons are injected into the cloud with a constant energy spectrum. While both of these options can in principle reproduce the observed behaviour (optical depth arguments aside) they require a specific set of conditions that are unlikely to be met in practice. Indeed, Marscher & Gear (1985) found that they could fit the variability of 3C 273 with a uniform expanding source model but only if ‘the injection of relativistic electrons was allowed to vary with radius in a rather ad hoc fashion’. They attributed the success of this model to its large number of free parameters. Arguing along similar lines, we do not consider that such models provide a convincing physical explanation for the phenomena observed in GRO J1655–40. Instead, given the obvious analogy between Galactic and extragalactic jet sources, we argue alternatively

that the variable radio emission arises in a small region behind a relativistic shock wave, and that the rise of the flare is driven by inverse-Compton cooling (cf. Marscher & Gear 1985). We note that the shock model developed by Kaiser et al. (2000) incorporates adiabatic and synchrotron cooling only and as such is mostly applicable to the decline of radio flares rather than to the rise phase discussed here.

3 GENERALISED SHOCK MODEL FOR EXTRAGALACTIC SOURCES

Spectral evolution during the flares of compact extragalactic radio sources can be explained by the generalised shock model of Marscher & Gear (1985). (For specific applications see e.g. Valtaoja et al. 1988 and Stevens et al. 1994, 1996, 1998). In the model, temporal evolution of the radio emission is divided into growth, plateau and decay stages (see the schematic illustration in Fig. 4). The emission region consists of relativistic jets along which transverse shocks propagate and accelerate electrons to relativistic energies. The shock waves form in response to changes in the conditions in the jet (such as pressure or velocities of the bulk flow). The evolution of the shock is described in terms of the flux density (S_ν) at the peak frequency (ν_m where $S_\nu[\nu_m] = S_m$) of the synchrotron spectrum where the opacity is close to unity. This point is fixed at any one time by the dominant energy-loss mechanism. When the emitting region is compact, inverse-Compton losses predominate (Compton or growth stage) but these fall off rapidly with radius as the shock expands and are superseded by synchrotron losses (synchrotron or plateau stage). As the shock expands further, the radiative lifetime of the electrons becomes large with respect to the time needed to traverse the emitting region and losses due to adiabatic expansion (adiabatic or decay stage) become more important. All three stages are approximated by power laws on the logarithmic (S_m, ν_m) plane. As the emitting region expands, ν_m is predicted to move to lower frequencies with time. S_m increases rapidly during the Compton stage, remains approximately constant during the synchrotron stage and decreases during the adiabatic stage.

The characteristics of spectral evolution predicted by the generalised shock model are summarised as follows (see Valtaoja et al. 1992 for more details). The maximum flare amplitude for any frequency on the Compton stage occurs when the spectrum transits onto the synchrotron stage. Light curves at such frequencies are thus predicted to peak simultaneously and because of the spectral shape, the flare amplitudes are expected to increase towards lower frequency – specifically, they should have the same power law form as the optically thin portion of the flare spectrum. Flare amplitudes at frequencies commensurate with the later stages are determined by the details of the spectral evolution, and are thus expected to be approximately constant during the synchrotron stage and to decrease during the adiabatic stage. The light curves will display time-lagged behaviour with a delay between any two frequencies equal to the time taken for the spectrum to evolve between them and become optically thin. Note that the development of the flare during the adiabatic stage is very similar to that predicted by the expanding cloud model, although, because the expansion is constrained to occur in a jet, the predicted time delays are shorter and the variation of flare amplitude with frequency is less pronounced.

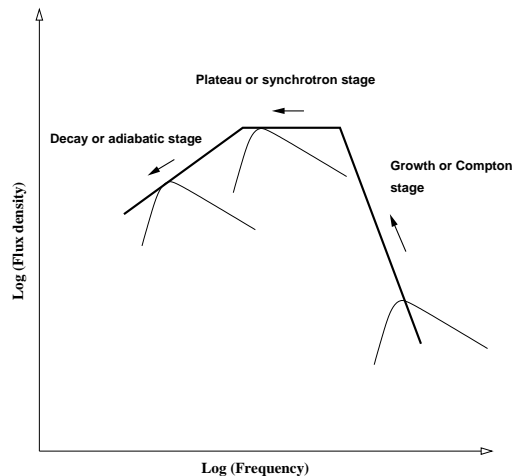


Figure 4. Schematic of flare spectral evolution according to the shock model of Marscher & Gear (1985). The thick solid line and arrows show the time evolution of the synchrotron self-absorption turn-over (S_m) as the shock expands along the jet.

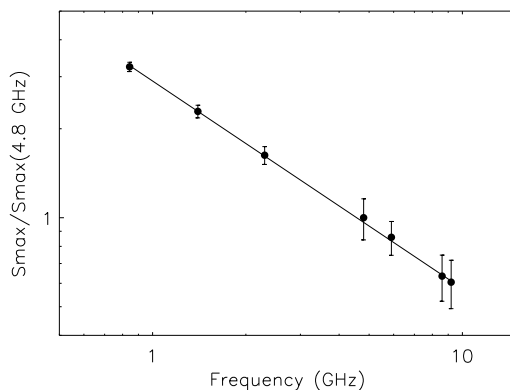


Figure 5. Flare amplitudes relative to 4.8 GHz. The slope of the fitted line is -0.70 ± 0.05

4 MICROQUASARS VS QUASARS

The generalised shock model prediction of simultaneously peaking emission at all frequencies coupled with flare amplitudes that increase towards lower frequencies (i.e. the Compton/growth stage) is consistent with the observations of GRO J1655–40 in 1994. According to the shock model, we would also expect the flare amplitudes to fall off as a power law since they should have the same frequency dependence as the spectrum of the flare when it reaches the transition point between the growth and plateau stages. In Fig. 5 we plot the flare amplitudes normalised to 4.8 GHz. A power law is clearly a good fit with a slope of -0.70 ± 0.05 , consistent with that expected for the optically thin portion of the flare synchrotron spectrum (cf. Stevens et al. 1996).

One apparent difference between the flaring behaviour of GRO J1655–40 and its extragalactic analogues, the blazars, is that the flare remains in the growth stage to much lower frequencies. For example, many of the sources in the sample considered by Stevens et al. (1994) show time delays between the 37 GHz, or occasionally the 90 GHz, emission and that at higher frequencies, although those authors noted that some BL Lacertae objects remained in the growth stage out to 4.8 GHz. An obvious contributor to this differ-

ence is the Doppler effect which will shift the emitted frequency of radiation in the jet frame, ν' , to a higher observed frequency, $\nu = \delta\nu'$. The relativistic Doppler factor, $\delta = \Gamma^{-1}(1 - \beta \cos \theta)^{-1}$ where $\Gamma = (1 - \beta^2)^{-1/2}$ is the bulk Lorentz factor, θ is the viewing angle and β is the jet speed in units of c . It is generally accepted that blazars have their jet axes oriented quite closely towards the observer; for example Teräsranta & Valtaoja (1994) find that blazars on average are aligned to within about 20 deg of the line-of-sight (see also Barthel et al. 1989). Estimates of Doppler factors for blazars range from extreme values of 0.005 to 33 with a mean value of around 5 (Guijosa & Daly 1996). The blazars with measured time delays from the sample of Stevens et al. (1994) have ‘inverse-Compton’ Doppler factors in the range 3.4–16 (see Guijosa & Daly 1996). The microquasar GRO J1655–40, however, is angled further towards the plane of the sky ($\theta = 70$ deg; Orosz & Bailyn 1997) and its estimated jet speed $\beta = 0.92$ (Hjellming & Rupen 1995) leads to $\delta \sim 0.6$. Higher values of the Doppler factor for blazars compared to that of GRO J1655–40 could thus easily lead to an order of magnitude difference in the frequency at which the flare exits the growth stage.

A second contributory factor might arise from physical differences between the jets of Galactic and extragalactic sources. Since the flare evolution is dependent on the photon energy density, the magnetic energy density and the lifetime of the emitting electrons compared to the time they take to cross the shock structure, two important parameters are the size of the emitting region and its magnetic field strength.

We can estimate the magnetic field from the flare decay time by assuming that the decay is radiative rather than expansion-loss driven. For the clear-cut case of a single flare we would expect the $1/e$ decay times, t , of the light curves to vary as $\nu^{-1/2}$ if radiative losses are the dominant energy-loss mechanism, or if adiabatic expansion losses predominate, then t will be the same at all frequencies. Unfortunately, the flaring behaviour that we observe is complex. At the monitoring frequencies presented in Fig. 1 the decay of the flares is interrupted by subsequent events, making it impossible to measure an accurate e-folding timescale. However, the multifrequency light curves presented by Hjellming & Rupen (1995) include data up to 22.5 GHz. For the flare in question, the decay of the 22.5 GHz lightcurve is more rapid than those at lower frequencies, most probably because the monitoring frequency is now sufficiently high that the e-fold timescale is similar to the interval between the bursts. This result provides evidence that synchrotron losses are driving the flux decay. If this is not the case then the implication would be that the synchrotron-loss stage is short lived or non-existent, as observed for 3C 273 (Stevens et al. 1998). The rest of this section assumes that the decay of the flare is driven by synchrotron losses. If this is not the case, and adiabatic expansion losses predominate then we will overestimate the magnetic field strength and underestimate the electron Lorentz factor and source extent.

For an e-fold decay timescale t and a peak frequency ν_m , the magnetic field is given by

$$B \sim 23 \delta^{-1/3} \left(\frac{\nu_m}{1 \text{ GHz}} \right)^{-1/3} \left(\frac{t}{5 \text{ day}} \right)^{-2/3} \text{ gauss}. \quad (1)$$

We estimated the flare decay time from the best sampled light curve (843 MHz). For the reasons discussed above this estimate is likely to be an upper limit but should not be out by more than a factor of two; using 5 d the estimated magnetic field strength is ~ 25 gauss. This value is approximately two orders of magni-

tude higher than typical estimates of 0.1–1 Gauss in extragalactic sources (e.g. Brown et al. 1989).

The Lorentz factor of the electrons emitting at 843 MHz is given by $\gamma \sim (2\pi m_e c \nu / e B)^{1/2} \sim 3.5$, where e and m_e are the electron charge and mass respectively. This value is approximately that required to explain the observed circular polarization as being intrinsic to the synchrotron radiation (Macquart et al. 2002) although the alternative mechanism, Faraday conversion, could also apply. In any case, we note that the presence of circularly polarized radiation is another characteristic that GRO J1655–40 shares with the blazars (see e.g. Wardle et al. 1998). Furthermore, strong evidence for our proposed model comes from the observed position angle of linear polarization at radio wavelengths which is very close to that of the jet direction (Hannikainen et al. 2000). For optically thin synchrotron radiation the implied magnetic field direction is perpendicular to the jet, as observed for many blazars (e.g. Cawthorne et al. 1993a,b), and as predicted by models in which a tangled component of magnetic field in the jet is compressed parallel to a transverse shock front (e.g. Hughes et al. 1989a).

Finally, we can estimate the source extent at the time when the spectrum transits from the growth stage onto the plateau stage. At this transition, the energy densities in particles (U_{ph}) and magnetic field are equal and thus so are the synchrotron and inverse-Compton lifetimes $t_{\text{syn}} = t_{\text{IC}}$. Using

$$t_{\text{IC}} \sim \frac{3 \times 10^7}{\gamma U_{\text{ph}}} \sim \frac{3 \times 10^7 c D^2}{\gamma \phi L} \text{ seconds}, \quad (2)$$

and assuming that, (1) the transition occurs when the 843 MHz light curve peaks (i.e. the flare amplitudes peak at this frequency), allowing us to use the values $t_{\text{IC}} = t_{\text{syn}} \sim 5$ d and $\gamma \sim 3.5$ deduced above, (2) the radiation field is produced by a central source of luminosity, $L \sim 10^{38}$ erg s $^{-1}$ and (3) that ϕ , a geometrical constant, is approximately unity, the calculated source size $D \sim 10^{13}$ cm. At a source distance of 3.2 kpc (Hjellming & Rupen 1995) this dimension translates to an angular size of about 0.2 mas. A 1.6 GHz VLBA map taken one day after the peak of the 843 MHz light curve shows a source of about 1 arcsec with a bright core and extended jets (Hjellming & Rupen 1995). Our proposed model requires that the radio flares originate in a small region close to the base of the jet as is observed in AGN.

5 FINAL REMARKS

We have shown that a model incorporating a propagating relativistic shock in a jet can qualitatively reproduce the multifrequency variability of GRO J1655–40. This model, which also fits the available polarization observations, is the canonical model used to explain the variability characteristics of extragalactic radio sources such as blazars. A detailed discussion of the applicability of this model to Galactic superluminal sources is beyond the scope of the present work, and in any case is limited by the availability of suitable data sets. It is important that other flares similar to the one discussed here are observed over a broad range of radio frequencies, and that they are first observed on the rising portion of the light curves. In this respect, we point out that the two sources discussed by Ball & Vlassis (1993), Nova Muscae 1991 and the Galactic Centre Transient, for which data were taken during the rise of the flares, both display the behaviour predicted by the Compton stage of the shock model. Both sources were observed to have an optically thin spectrum during the rising phase of the outburst which can be accommodated by the Compton stage if the self-absorption turnover

had already passed the lowest observing frequency when the flux monitoring began.

ACKNOWLEDGMENTS

J.A.S. and D.C.H. acknowledge support from PPARC, and K.W. acknowledges support from the Australian Research Council through an Australian Research Fellowship. D.C.H. also acknowledges travel support from the Academy of Finland, and thanks the University of Sydney and Jodrell Bank for their hospitality and financial support during her visits.

REFERENCES

- Ball L., Vlassis M., 1993, *PASA*, 10, 342
 Barthel P.D., 1989, *ApJ*, 336, 606
 Brown L.M.J., et al., 1989, *ApJ*, 340, 129
 Cawthorne T.V., Wardle J.F.C., Roberts D.H., Gabuzda D.C., 1993b, *ApJ*, 416, 519
 Cawthorne T.V., Wardle J.F.C., Roberts D.H., Gabuzda D.C., Brown L.F., 1993a, *ApJ*, 416, 496
 Edelson R.A., Krolik J.H., 1988, *ApJ*, 333, 646
 Fender R.P., 2001, *AP&SSS*, 276, 69
 Fender R.P., 2002, in eds. A.W. Guthman, M. Georganopoulos K. Manolakou and A. Macrowith, “Relativistic outflow in astrophysics”, Springer lecture notes in physics, (Berlin, Springer-Verlag), in press
 Gaskell C.M., Peterson B.M., 1987, *ApJS*, 65, 1
 Greiner J., Cuby J.G., McCaughrean M.J., Castro-Tirado A.J., Mennickent R.E., 2001, *A&A*, 373, L37
 Gujosa A., Daly R.A., 1996, *ApJ*, 461, 600
 Han X., Hjellming R. M., 1992, *ApJ*, 400, 304
 Hannikainen D.C., Hunstead R.W., Wu K., McKay D.J., Smits D.P., Sault R.J., 2000, *ApJ*, 540, 521
 Hjellming R.M., Johnston K.J., 1988, *ApJ*, 328, 600
 Hjellming R.M., Rupen M.P., 1995, *Nature*, 375, 464
 Hughes P.A., Aller H.D., Aller M.F., 1985, *ApJ*, 298, 310
 Hughes P.A., Aller H.D., Aller M.F., 1989a, *ApJ*, 341, 54
 Hughes P.A., Aller H.D., Aller M.F., 1989b, *ApJ*, 341, 68
 Hunstead R., Campbell-Wilson D., McKay D., Lovell J., Kesteven M., 1994, *IAUC*, 6062
 Kaiser C.R., Sunyaev R., Spruit H.C., 2000, *A&A*, 356, 975
 Macquart J.-P., Wu K., Sault R.J., Hannikainen D.C., 2002, *A&A*, 396, 615
 Marscher A.P., Gear W.K., 1985, *ApJ*, 298, 114
 Mirabel I.F., Rodriguez L.F., 1994, *Nature*, 371, 46
 Mirabel I.F., Rodriguez L.F., 1998, *Nature*, 392, 673
 Mirabel I.F., Rodriguez L.F., 1999, *ARA&A*, 37, 409
 Orosz J.A., Bailyn C.D., 1997, *ApJ*, 477, 876
 Pauliny-Toth I.I.K., Kellermann K.I., 1966, *ApJ*, 146, 634
 Reynolds J., et al., 1994, *IAUC*, 6063
 Shklovsky I.S., 1965, *SvA.*, 7, 748
 Soria R., Wickramasinghe D.T., Hunstead R.W., Wu K., 1998, *ApJ*, 495, L95
 Stevens J.A., Litchfield S.J., Robson E.I., Hughes D.H., Gear W.K., Teräsraanta H., Valtaoja E., Tornikoski M., 1994, *ApJ*, 437, 91
 Stevens J.A., Litchfield S.J., Robson E.I., Cawthorne T.V., Aller M.F., Aller H.D., Hughes P.A., Wright M.C.H., 1996, *ApJ*, 466, 158
 Stevens J.A., Robson E.I., Gear W.K., Cawthorne T.V., Aller M.F., Aller H.D., Teräsraanta H., Wright M.C.H., 1998, *ApJ*, 502, 182
 Teräsraanta H., Valtaoja E., 1994, *A&A*, 283, 51
 Tingay S.J. et al., 1995, *Nature*, 374, 141
 Valtaoja E. et al., 1988, *A&A*, 203, 1
 Valtaoja E., Teräsraanta H., Urpo S., Nesterov N.S., Lainela M., Valtonen M., 1992, *A&A*, 254, 71
 van der Laan H., 1966, *Nature*, 211, 1131
 Wardle J.F.C., Homan D.C., Ojha R., Roberts D.H., 1998, *Nature*, 395, 1